Controlling the Energy Transfer in Dipole Chains

Jeroen J. de Jonge,[†] Mark A. Ratner,*[,†] Simon W. de Leeuw,[‡] and Richard O. Simonis[‡]

Department of Chemistry, Northwestern University, 2145 Sheridan Road, Evanston, Illinois 60208, and Physical Chemistry and Molecular Thermodynamics, DelftChemTech, Delft University of Technology, Julianalaan 136, 2628 BL, Delft, The Netherlands

Received: June 2, 2005; In Final Form: August 1, 2005

Processing digital signals on the molecular scale is of great interest. In this paper, we discuss the control of pulselike energy propagation through one-dimensional arrays of dipoles. Three systems are explored. In the first system, a chain of coaxial dipoles is gated by two control dipoles. Changing the orientation of these control dipoles lets us control the transfer of energy in the chain. In the other two systems, the chain−branch system and the two-branch system, two chains are used as an input and the propagation of energy is controlled by sending one or two signals toward the junction. Both systems can operate as a logical AND port. Their geometrical configurations are key to a well-defined control and operation of the AND port.

1. Introduction

Molecular scale machines are of current interest in many areas.[1,2] There are models concerning the use of one or more molecules to process digital signals,[3] such as linear wires,[4−6] transistor-like switches,[7,8] and logic gates.[9−12] Recent simulations[13] suggest that energy can be transferred through a linear chain of classical point dipoles in a pulselike fashion using their dipole−dipole interactions. In these simulations, the classical point dipoles represent molecules that have a (di)polar rotor, such as the ones synthesized and characterized by Garcia-Garibay et al.[14,15] and Michl et al.[16−18] This paper presents results showing that a logical "AND" gate consisting of such chains can be created.

The dipolar molecular rotors are molecules that consist of a stand and a dipolar rotor, connected by a rotation axis that may most simply be a C−C or a Si−C bond. Two types of molecules have been proposed: the so-called azimuthal rotors that rotate in planes parallel to the surface they are mounted on[17,19] and altitudinal rotors that rotate perpendicular to the surface.[18]

Feedback-controlled lithography,[20] which makes it possible to bind covalently molecules at a specific point on a Si surface, and the various types of "Tinkertoy" construction sets[21,22] have made it possible to build both single-molecule and two-dimensional (2D) structures on surfaces that can include molecules with dipolar rotor parts.

The strongest interaction between these types of molecules at reasonable distances (15−25 Å) is the dipole−dipole interaction between the dipolar rotors. Electrostatic interactions in 2D lattices, and especially dipole−dipole interactions, have been studied extensively by Rozenbaum.[23−27] The dipole−dipole interactions are mainly responsible for creating stable, orientationally ordered structures of polar molecules.[24−26] Dispersion relations and orientational structures in triangular, square, and honeycomb lattices were obtained.[26,27] In the honeycomb lattice, vortex configurations of dipoles have been shown to be formed in the lattice plane.

Computational papers have examined interactions of individual dipolar molecular rotors with an electric field[17] as well as interactions within one-dimensional dipole chains. We have examined low-energy excitation properties in two types of chains:[28,29] In the first type, the dipoles all rotate around the same axis, this is therefore called the coaxial chain. In the second type, the dipoles all rotate in the same plane, the coplanar chain. It was also shown that upon exciting the first dipole in a chain of (coaxial or coplanar) dipoles can initiate a low-temperature transfer of a pulselike energy packet through that chain.[13] Exciting the first dipole was done by giving it an instantaneous "kick".

In this paper, we propose and discuss three structures that allow the control of the energy transfer through a coaxial chain. The energy transfer in the chain depends mainly on the ability of the dipoles to rotate and "pass" the energy. In the structures described below, single dipoles and short chains of dipoles are used to lower or raise the rotational potential barrier of one of the dipoles in the chain and thereby to control the energy transfer through that chain.

The first structure **A** consists of a 25-dipole coaxial chain and two control dipoles which form a gate (Figure 1A). The two control dipoles are positioned on either side of the 13th dipole. They are fixed in their positions and orientations during the (computational) experiment. By orienting the control dipoles in different ways, we can open or close the gate for energy transfer (Figure 1B). In the first orientation (i), the control dipoles are in line with the gated (junction) dipole. In this orientation, the rotational potential energy barrier of the junction dipole has its maximum height and the junction dipole is strongly hindered in its rotational motion: the gate is closed. In the other orientations (ii and iii), the control dipoles are rotated over 90° such that their combined interaction with the chain is zero. Now, the rotational potential barrier height is unperturbed and the signal can pass unhindered: the gate is open.

The second structure **B** consists of a chain of 36 coaxial dipoles and a branch of 10 coaxial dipoles that is close to the 11th (junction) dipole with angle α at a distance d (Figure 2). The addition of this branch raises the rotational potential barrier height of the junction dipole and thus hinders the transfer of energy through the junction. We will show that if we also excite the branch, in the same way as the chain, then the energy can be transferred unhindered for some geometrical configurations. The geometrical variables are angle α and distance d.

* To whom correspondence should be addressed. E-mail: ratner@chem.northwestern.edu.
[†] Northwestern University.
[‡] Delft University of Technology.

10.1021/jp0529523 CCC: $33.50
Published on Web 12/07/2005

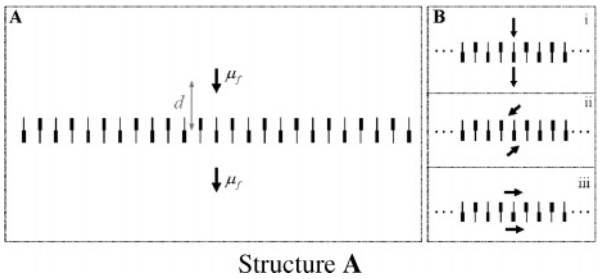

Figure 1. (A) Coaxial dipole chain is gated by two control dipoles μ_f at a distance d. (B) The control dipoles can be set in the closed position (i) or in an open position (ii and iii).

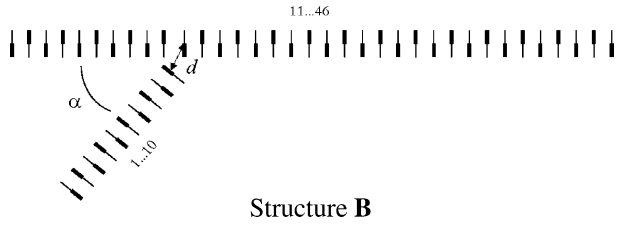

Figure 2. Branch of 10 coaxial dipoles is attached to a 36 dipole chain under an angle α at distance d. One can excite only the chain or both the chain and the branch. The dipoles are indexed according to the numbers next to the branches.

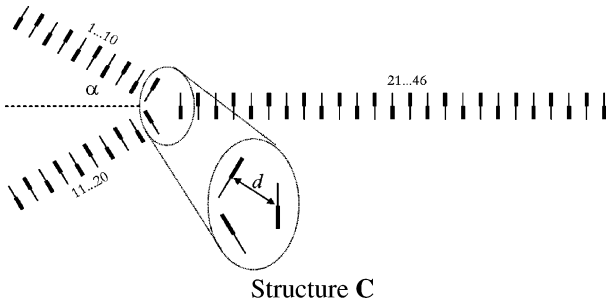

Figure 3. System consists of two branches and a chain. The geometrical variables are a half angle α between the left branches and the distance d as defined in the enlargement.

The third structure **C** consists of two branches (each 10 dipoles) that come together under an angle α and merge into a chain (26 dipoles) (Figure 3). The incoming branches are separated a distance d from the chain. The transfer of energy through the junction can be controlled by exciting either one or both of the branches. The geometric variables are again α and d.

We characterize these structures using molecular dynamics (MD) simulations. We excite one or more dipoles and monitor the energy pulse as it travels through the structures. As a measure of transferred energy, we define E_T as the maximum kinetic energy of the last dipole in the chain when the energy pulse reaches it. For each structure, its variables are optimized to create structures that have the best control of the energy transfer E_T.

2. Simulation Methods

Molecular dynamics calculates the trajectory of the system, that is, the orientations of the dipoles and their rotational velocities at discrete points in time. In this paper, the dipolar rotors are represented as classical point dipoles that interact with each other according to the (long-ranged) dipole−dipole pair potential V_{ij}

$$V_{ij}(\vec{r}_{ij}) = -\frac{1}{4\pi\epsilon_0}\left[\frac{\vec{\mu}_i\cdot\vec{\mu}_j}{r_{ij}^{\,3}} - 3\frac{(\vec{\mu}_i\cdot\vec{r}_{ij})(\vec{\mu}_j\cdot\vec{r}_{ij})}{r_{ij}^{\,5}}\right] \qquad (1)$$

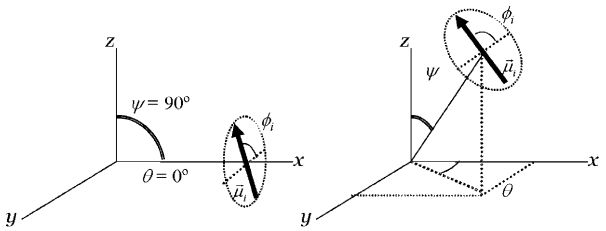

Figure 4. Angle ϕ is defined as the rotation around the x-axis, if the dipole rotates in the xy-plane. The right figure shows the transformation from polar to Cartesian coordinates according to the matrix $\mathbf{T}_i$ if the rotation axis is differently oriented.

in which $\vec{\mu}_i$ is the ith dipole moment, $\vec{r}_{ij}$ is the center-to-center vector between dipoles i and j, and $r_{ij} = |\vec{r}_{ij}|$. The dipoles are limited to rotation around their centers in one plane, and they all have a constant and equal dipole moment $|\vec{\mu}_i| = \mu_0$ and moment of inertia $I_i = I_0$. The interdipole distance for neighbors is equidistant on each branch, $r_{ij} = |i - j|r_0$.

We can write the dipole moments $\vec{\mu}_i$ and their time derivatives $\dot{\vec{\mu}}_i$ in terms of their only degree of freedom, angle ϕ_i

$$\vec{\mu}_i = \mu_0\mathbf{T}_i(\cos\phi_i, \sin\phi_i) \qquad (2)$$

$$\dot{\vec{\mu}}_i = \mu_0\mathbf{T}_i(-\sin\phi_i, \cos\phi_i)\dot{\phi}_i \qquad (3)$$

where $\mathbf{T}_i$ transforms the polar coordinates to Cartesian coordinates

$$\mathbf{T}_i = \begin{pmatrix} \cos\theta_i\cos\psi_i & -\sin\psi_i \\ \sin\theta_i\cos\psi_i & \cos\psi_i \\ -\sin\theta_i & 0 \end{pmatrix} \qquad (4)$$

Angles θ_i and ψ_i of eq 4 are defined in Figure 4. Note that θ_i and ψ_i do not change in time, and thus matrix $\mathbf{T}_i$ is constant during the simulation.

The Lagrangian L of a system of N dipoles is written as

$$L = \sum_{i=1}^{N}\frac{I_i\dot{\vec{\mu}}_i}{2|\vec{\mu}_i^{\,2}|} - \frac{1}{4\pi\epsilon_0}\sum_{i=1}^{N-1}\sum_{j=i+1}^{N}\left[\frac{\vec{\mu}_i\cdot\vec{\mu}_j}{r_{ij}^{\,3}} - 3\frac{(\vec{\mu}_i\cdot\vec{r}_{ij})(\vec{\mu}_j\cdot\vec{r}_{ij})}{r_{ij}^{\,5}}\right] \qquad (5)$$

in which $\dot{\mu}_i$ and $\vec{\mu}_i$ can be written with eqs 2 and 3 in terms of ϕ_i and $\dot{\phi}_i$. Using the Euler−Lagrange equation

$$\frac{\mathrm{d}}{\mathrm{d}t}\left(\frac{\partial L}{\partial\dot{\phi}_i}\right) = \frac{\partial L}{\partial\phi_i} \qquad (6)$$

on eq 5 the following equations of motion can be found for dipoles i, $i = 1, ..., N$

$$I_0\ddot{\phi}_i = -\frac{1}{4\pi\epsilon_0}\sum_{j=1,j\neq i}^{N}\left[\frac{\vec{\mu}_i^{\,*}\cdot\vec{\mu}_j}{r_{ij}^{\,3}} - 3\frac{(\vec{\mu}_i^{\,*}\cdot\vec{r}_{ij})(\vec{\mu}_j\cdot\vec{r}_{ij})}{r_{ij}^{\,5}}\right] \qquad (7)$$

where $\vec{\mu}_i^{\,*}$ is the derivative of $\vec{\mu}_i$ with respect to ϕ_i

$$\vec{\mu}_i^{\,*} = \frac{\partial\vec{\mu}_i}{\partial\phi_i} = \mu_0\mathbf{T}_i(-\sin\phi_i, \cos\phi_i) \qquad (8)$$

With this representation of the dipole moment, it is not necessary to use constraint dynamics,[28] which has larger errors and requires more computation time. From the initial conditions the trajectory of the system is calculated, integrating the equations of motion using the velocity Verlet algorithm.[30]

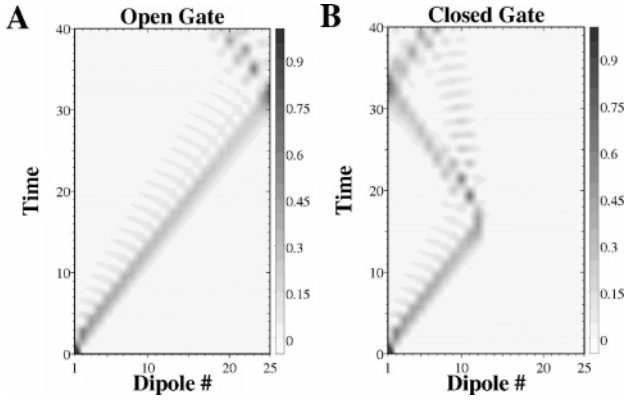

Figure 5. Kinetic energy (intensity) of the individual dipoles in time for a gated chain in the open (A) and closed (B) configuration.

Each system starts in the ground state in every simulation, so that there are no sources of kinetic energy other than the excitation. The chain and branches are excited by giving the first dipole an initial "kick", $\dot{\phi}_0$, while the rest of the chain is at rest.

Reduced Units. Reduced units[13,28] are used to keep the model applicable for more than one molecule type. The parameters μ_0, I_0, and r_0 are set equal to 1 as is the electrostatic prefactor $(1/4\pi\epsilon_0)$. Substitution of the actual dipole moment and moment of inertia of the molecule and the interdipole distance values results in real units.

As an example, we use parameters of the altitudinal dipolar rotor no. **11** from ref 18. This molecule has a dipole moment $\mu_0 = 3.7$ D and a moment of inertia $I_0 = 1150$ amu Å^2. A (realistic) interdipole distance of 20 Å is assumed. The real quantities E and t can be calculated from their unitless reduced units E^* and t^* with

$$E = E^* \frac{{\mu_0}^2}{4\pi\epsilon_0 {r_0}^3} \tag{9}$$

$$t = t^* \sqrt{\frac{4\pi\epsilon_0 I_0 {r_0}^3}{{\mu_0}^2}} \tag{10}$$

Now every reduced time unit $t^* = 1$ corresponds to $t = 10.56$ ps, and every reduced energy unit $E^* = 1$ corresponds with $E = 0.431$ kcal/mol.

3. Results and Discussion

A. Gated Chain. Simulations are done on systems with the gate open and with the gate closed. The control dipoles are positioned at a distance equal to the interdipole distance in the chain, $d = 1.0$, and the magnitude of the dipole moment is the same as that of the dipoles in the chain, $\mu_f = 1.0$. The excitation is an initial rotational velocity of $\dot{\phi}_0 = 2.0$. If the gate is open (configuration iii of Figure 1B is used), then the energy pulse travels through the gate unhindered (see Figure 5A). The result is the same as if the gate was not there at all. The maximum kinetic energy of the last dipole in the chain, as the pulse reaches it, is $E_T = 0.849$ after 32 time units.

The gate is closed by rotating the dipoles over 90°. Now, as the signal reaches the gate, most of the signal is reflected back (Figure 5B). With the gate closed, the energy transfer is much lower, $E_T = 0.043$, or 5% of the unhindered E_T.

The maginitude of the control dipole moments μ_f and the distance to the chain d are very important for the efficiency of

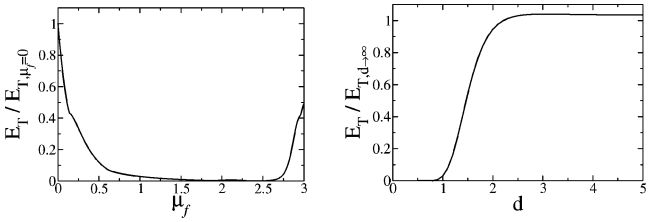

Figure 6. Energy transfer E_T, relative to the unhindered result, vs the control dipole moment μ_f (A) and the distance d to the chain (B). The configuration in Figure 1A is assumed.

blocking the energy pulse. Figure 6A plots E_T (relative to the unhindered result) as a function of μ_f ($d = 1.0$). The graph shows that for $\mu_f = 0.11$, E_T is already half of the unhindered result and for $\mu_f = 0.5$, only 12% of the unhindered E_T is transferred. For large control dipole moments ($\mu_f > 2.6$), the energy transfer increases again. This is caused by the interaction between the control dipoles and the dipoles neighboring the junction dipole. For large μ_f values, the dipoles neighboring the junction dipole have a stronger interaction with the control dipoles than with the junction dipole, but their orientation is such that that interaction has a potential maximum. Rotation of these neighboring dipoles over 180° to their (new) potential minimum starts a kinetic energy pulse. It is this energy pulse that is recorded for $\mu_f > 2.6$ and not the excitation. If, for $\mu_f > 2.6$, the simulation starts with the junction dipole and its two neighbors parallel to each other (potential minimum), then the energy transfer is zero.

If the control dipoles are positioned further away, then the blocking efficiency decreases (E_T increases, Figure 6B), and if they are positioned closer, then the efficiency increases (E_T decreases). Figure 6B plots E_T as a function of distance d. The graph shows that E_T increases fast if the d value is increased, up until the unhindered value. E_T is 50% of the unhindered transfer for $d = 1.5$, and E_T is 90% for $d = 2.0$.

The interaction energy between a control dipole and a dipole in the chain depends on the control dipole moment (μ_f) and the distance (r_{f_i}) according to (see eq 1)

$$V_{f_i} \propto \frac{\mu_i \mu_f}{{r_{f_i}}^3} \tag{11}$$

Any increase in distance requires a cubed increase in dipole moment to obtain the same result. To prevent unwanted sources of kinetic energy, the magnitude of μ_f is limited such that the interaction with the dipoles neighboring the junction dipole is not dominant (if $d = 1.0$ then $\mu_f < 2.6$).

Using fixed dipoles to control the energy transfer through a chain is very effective. However, synthetic structuring of the orientation of the control dipoles might be difficult.

B. Chain with Branch. Simulations on this structure are done both by exciting only the chain and by exciting the chain and the branch. If both the chain and the branch are excited, then the direction of the initial rotational velocity is taken in the same direction. In that case, both excitations reach the junction at the same time. Both angle α and distance d are varied to find the maximum difference between chain only and chain and branch excitation energy transfers. If there is no branch, and the chain is excited with $\dot{\phi}_0 = 2.0$, then the energy transfer is $E_T = 0.714$. As an example, we look at the system with $\alpha = 45°$ and $d = 1.8$. If only the chain is excited, then part of the energy pulse is reflected at the junction and part is transferred (see Figure 7A). The energy transfer is $E_T = 0.482$ or 67% of the *unbranched* chain. If both the chain and the branch are excited (Figure 7B), then $E_T = 0.771$ or 108% of the unbranched

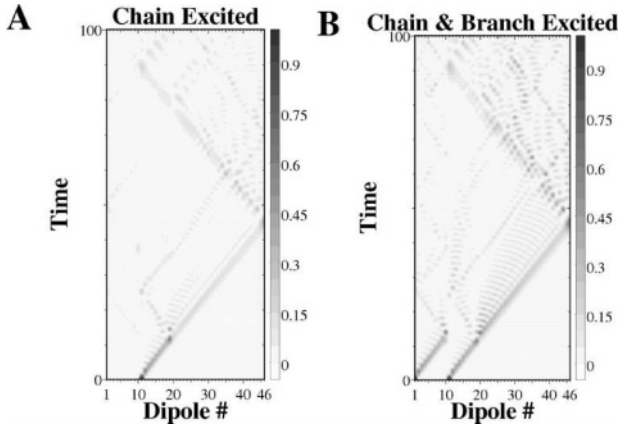

Figure 7. Kinetic energy (intensity) of the individual dipoles (indexed according to Figure 2 on the horizontal axis) in time for the chain with the branch system in case only the chain is excited (A) and in case both chain and branch are excited (B): $\alpha = 45°$, $d = 1.8$, $\dot{\phi}_0 = 2.0$.

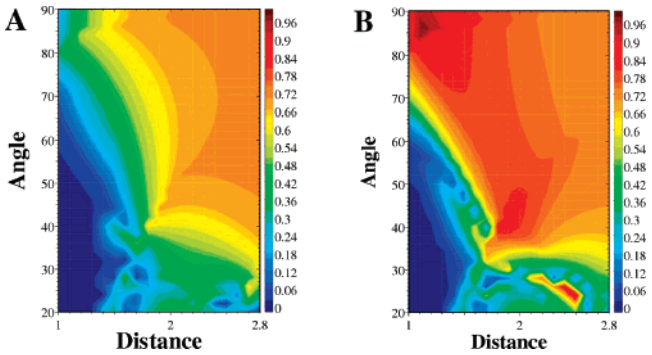

Figure 8. Energy transfer E_T (color) as a function of α and d in case only the chain is excited (A) and the chain and branch are simultaniously excited (B).

chain. The extra excitation of the branch helps the energy transfer. However, the difference between the two cases is not very large, only a factor 1.6, so it would be hard to measure a difference.

The same calculations are repeated for $20° \leq \alpha \leq 90°$ in steps of 2° and $1.0 \leq d \leq 2.8$ in steps of 0.1. Their energy transfers E_T are plotted in color in Figure 8. Mostly, the extra excitation of the branch does not lead to a substantial increase in the energy transfer, but for some configurations, the difference is considerable. Figure 8B has a maximum of 0.964 for $\alpha = 88°$ and $d = 1.2$. In the same configuration, the system with only the excited chain produces an output of 0.309, smaller by approximately a factor of 3. The largest difference in E_T occurs for $\alpha = 90°$ and $d = 1.0$: E_T values are then 0.875 and 0.180, almost a factor of 5. However, small changes in the geometry lead to large changes in the output.

This system can, if in the right geometrical configuration, act as a logical "AND" port. If only the chain is excited, then the energy transfer is low. If both the chain and the branch are excited, then the output is roughly three to five times larger.

C. Two Branches. Simulations are done with one branch excited and with both branches excited. If both branches are excited, then they are excited in the same direction such that their interactions with the chain do not cancel out and they are excited at the same time such that both energy pulses reach the junction at the same time.

Figure 9 shows the kinetic energy of the individual dipoles in time for both situations for $\alpha = 48°$, $d = 1.2$, and $\dot{\phi}_0 = 2.0$. The graph for a single excited branch shows that most of the energy pulse is reflected back in the branch and only a small

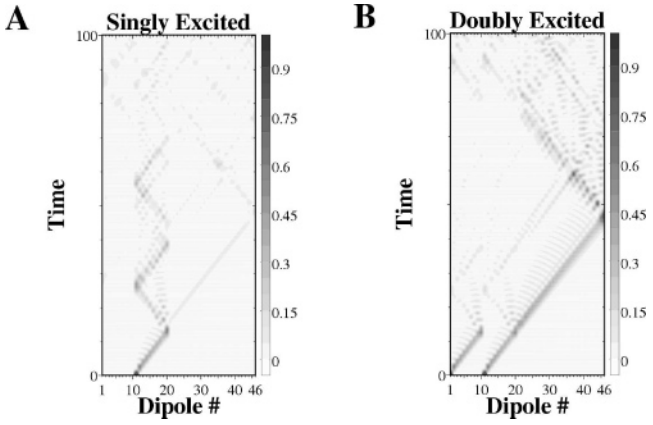

Figure 9. Kinetic energies (intensity) of the individual dipoles (indexed according to Figure 3 on the horizontal axis) vs the time for a singly (A) and a doubly (B) excited system: $\alpha = 48°$, $d = 1.2$, $\dot{\phi}_0 = 2.0$.

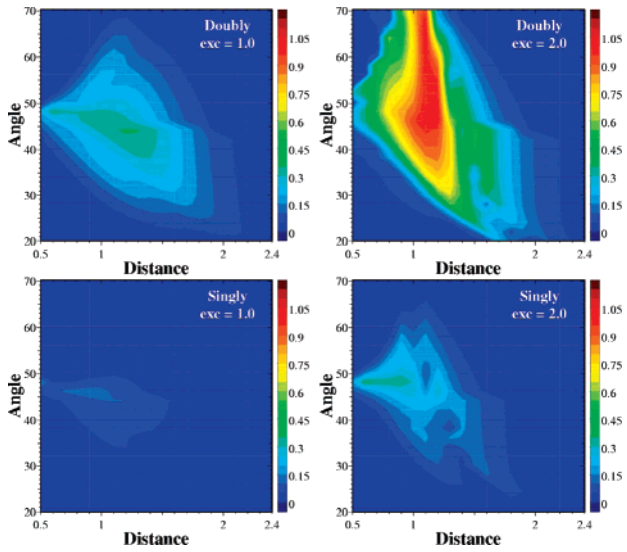

Figure 10. Energy transfer E_T as a function of α and d for singly and doubly excited systems for two excitations: $\phi_0 = 1.0$ and 2.0.

part is transferred, $E_T = 0.260$. For two excited branches, the energy transfer is considerably higher, $E_T = 1.025$.

These calculations are repeated for $20° \leq \alpha \leq 70°$ in steps of 2° and $0.5 \leq d \leq 2.4$ in steps of 0.1 for excitations $\dot{\phi}_0 = 1.0$ and 2.0. The results are shown in the graphs of Figure 10. A larger excitation leads to higher energy transfers. The difference between singly and doubly excited systems is the largest for $\alpha = 48°$ and $d = 1.2$ (see for values above), approximately a factor of 4. The result of a doubly excited system is not simply an addition of two singly excited ones: The energy transfer quadruples if the extra branch is excited.

As can be seen in Figure 10, the magnitude of the excitation plays an important role. Simulations are done by varying the excitation for systems with $\alpha = 48°$ and $d = 1.2$ for singly and doubly excited systems. Figure 11 plots E_T vs $\dot{\phi}_0$ and shows that the energy transfer increases more for doubly excited systems than for singly excited systems. For excitations $\dot{\phi}_0 > 2.3$, the energy transfer through the branches is not straightforward anymore[13] because of a dynamic bottleneck. The excitation of the first dipole in the chain is not directly followed by its neighbor, and the signal is not pulselike and is very broad. This leads to erratic behavior in this two-branch system and in some (unpredictable) situations to an increase in energy transfer. The peaks shown in Figure 10 do not exist for other geometries α and d.

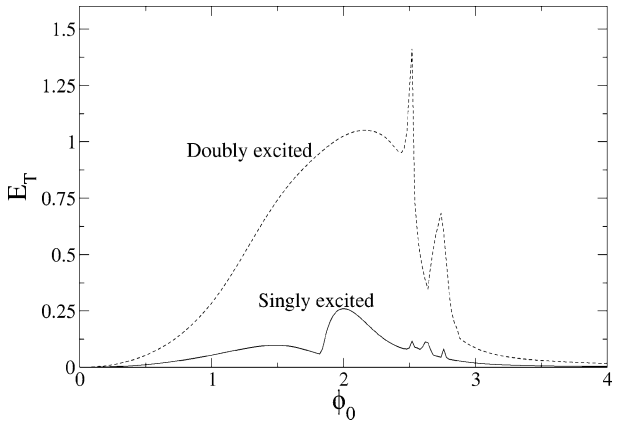

Figure 11. E_T as a function of the excitation $\dot{\phi}_0$ for singly excited (solid line) and doubly excited (dashed line) systems.

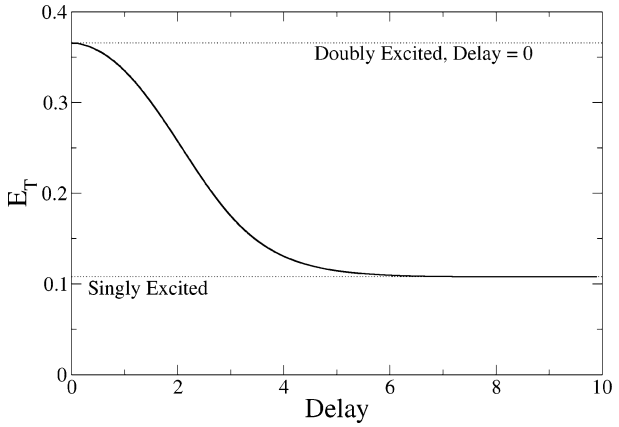

Figure 12. Energy transfer E_T as a function of the delay between the excitations of the input branches: $\alpha = 45°$, $d = 1.2$, $\dot{\phi}_0 = 1.0$.

To understand the importance of both excitations arriving at the same time at the junction, simulations are done in which a delay between the two excitations is implemented. Figure 12 shows that the energy transfer falls off fast if a delay is introduced. A delay of 2 time units results in a 50% loss in energy transfer, and if the delay is more than 5 time units, the response is the same as if only one branch was excited.

If the system is reversed and the last dipole of the chain is excited, then an energy pulse starts traveling from the end of the chain toward the junction with the two branches. At the junction most of the energy is reflected back into the chain, and a small part is transferred, and equally divided over the two branches. The energy transfer is $E_T = 0.148$ and smaller than that of the singly excited system ($\alpha = 45°$, $d = 1.2$).

Again, the energy transfer is very sensitive to an accurate geometry of the system. Small deviations from the optimal configuration can lower the difference betwen doubly and singly excited systems from a factor of 4 to a factor of 2 or lower. This system also can, if in the right geometrical configuration, act as a logical "AND" port. If two branches are excited, then the output is consirably higher than if only one branch was excited.

4. Summary

We have modeled three systems in which the rotational energy transfer through coaxial dipole chains can be controlled. In the first system, a chain was gated by two control dipoles. Orienting the dipoles in a certain direction let us successfully open and close the gate for energy transfer. If the gates can be placed close enough to the chain and their orientation can be controlled, then this becomes an effective way to block or transfer the energy through a chain of dipoles.

In the other two systems, branches were added to the system. For certain geometrical configurations, we could control the energy transfer by exciting both branches or only one of them. The systems can operate as logical "AND" ports. Increasing the magnitude of the excitation (up to a certain value) leads to larger E_T values. However, these systems are very sensitive to the accuracy of the geometrical configuration. Also, in case two branches were excited, it was shown that these excitations have to be sufficiently close together (in time), otherwise the energy transfer drops fast.

Acknowledgment. We are grateful to Josef Michl for useful suggestions and to the ARO for support under the MURI program.

References and Notes

(1) Balzani, V.; Credi, A.; Venturi, M. *Molecular Devices and Machines—A Journey into the Nano World*; Wiley-VCH: Weinheim, Germany, 2003.
(2) Sauvage, J.-P., Ed. *Molecular Machines and Motors*; Springer: Berlin, Germany, 2001.
(3) Joachim, C.; Gimzewski, J. K.; Aviram, A. *Nature* **2000**, *408*, 541.
(4) Aviram, A.; Ratner, M. A. *Chem. Phys. Lett.* **1974**, *29*, 277.
(5) Chiang, C. K.; Druy, M. A.; Gau, S. C.; Heeger, A. J.; Louis, E. J.; MacDiamid, A. G.; Park, Y. W.; Shirakawa; H. *J. Am. Chem. Soc.* **1978**, *100*, 1013.
(6) Reed, M. A.; Zhou, C.; Muller, J.; Burgin, T. P.; Tour, J. M. *Science* **1997**, *278*, 252.
(7) Tans, S. J.; Verschueren, A. R. M.; Dekker, C. *Nature* **1998**, *393*, 49.
(8) Di Ventra, M.; Pantelides, S. T.; Lang; N. D. *Appl. Phys. Lett.* **2000**, *78*, 3448.
(9) Birge, R. R.; Lawrence, A. F.; Findsen, I. A. In *Proceedings of the International Congress on Technology & Technology Exchange 3−8*; International Technology Institute: Pittsburgh, PA, 1986.
(10) Credi, A.; Balzani, V.; Langford, S. J.; Stoddart, J. F. *J. Am. Chem. Soc.* **1997**, *119*, 2679.
(11) De Silva, A. P.; McClenaghan, N. D. *J. Am. Chem. Soc.* **2000**, *12*, 3965.
(12) Collier, C. P.; Wong, E. W.; Belohradsky, M.; Raymo, F. M.; Stoddart, J. F.; Kuekes, P. J.; Williams, R. S.; Heath, J. R. *Science* **1999**, *285*, 391.
(13) De Jonge, J. J.; Ratner, M. A.; De Leeuw, S. W.; Simonis, R. O. *J. Phys. Chem. B* **2004**, *108*, 2666.
(14) Dominguez, Z.; Khuong, T.-A. V.; Dang, H.; Sanrame, C. N.; Nunez, J. E.; Garcia-Garibay, M. A. *J. Am. Chem. Soc.* **2003**, *125*, 8827.
(15) Godinez, C. E.; Zepeda, G.; Mortko, C. J.; Dang, H.; Garcia-Baribay, M. A. *J. Org. Chem.* **2003**, *69*, 1652.
(16) Clarke, L. I.; Horinek, D.; Kottas, G. S.; Varaska, N.; Magnera, T. F.; Hinderer, T. P.; Horansky, R. D.; Michl, J.; Price, J. C. *Nanotechnology* **2002**, *13*, 533.
(17) Horinek, D.; Michl, J. *J. Am. Chem. Soc.* **2003**, *125*, 11900.
(18) Zheng, X.; Mulcahy, M. E.; Horinek, D.; Galeotti; F.; Magnera, T. F.; Michl, J. *J. Am. Chem. Soc.* **2004**, *126*, 4540.
(19) Hou, S.; Sagara, T.; Xu, D.; Kelly, T. R.; Ganz, E. *Nanotechnology* **2003**, *14*, 566.
(20) Hersam, M. C.; Lee, J.; Guisinger, N. P.; Lyding, J. W. *Superlattices Microstruct.* **2000**, *27*, 583.
(21) Michl, J.; Magnera, T. F. *Proc. Natl. Acad. Sci.* **2002**, *99*, 4788.
(22) Schwab, P. F. H.; Noll, B. C.; Michl, J. *J. Org. Chem.* **2002**, *67*, 5476.
(23) Rozenbaum, V. M.; Ogenko, V. M. *Fiz. Tverd. Tela (Leningrad)* **1984**, *26*, 1448; *Sov. Phys. Solid State* **1984**, *26*, 887.
(24) Mazolvskii, Y. M.; Rozenbaum, V. M. *Physica A* **1991**, *175*, 121.
(25) Rozenbaum, V. M. *Zh. Eksp. Teor. Fiz.* **1991**, *99*, 1836; *JETP* **1991**, *72*, 1028.
(26) Rozenbaum, V. M. *Phys. Rev. B* **1995**, *51*, 1290.
(27) Rozenbaum, V. M. *Phys. Rev. B* **1996**, *53*, 6240.
(28) De Leeuw, S. W.; Solvaeson, D.; Ratner, M. A.; Michl, J. *J. Phys. Chem. B* **1998**, *102*, 3876.
(29) Sim, E.; Ratner, M. A.; De Leeuw, S. W. *J. Phys. Chem. B* **1999**, *103*, 8663.
(30) Swope, W. C.; Andersen, H. C.; Berens, P. H.; Wilson, K. R. *J. Chem. Phys.* **1982**, *76*, 637.